

Fast Indirect GMPPT Method for PV Systems under Uniform and Partial Shading Conditions



K. Ameer¹, A. Hadjaissa^{1*}, N. Abouchabana¹, A. Rabehi²

¹LACoSERE Laboratory, University Amar Telidji of Laghouat Laghouat, Algeria

²MIS Laboratory. University of Picardie Jul. Verne, 33 rue Saint Leu.80039 Amiens Cedex1, France



ABSTRACT: Under Partial Shading Conditions (PSCs), conventional MPPT techniques fail to locate the Global Maximum Power Point (GMPP) for PV generators, and when PSCs change suddenly and repetitively, several GMPP tracking techniques takes time to find or miss the target. To overcome these shortcomings, this paper proposes a new and fast technique that can identify and catch very quickly the GMPP. Due to the use of a PID controller, the PV system is improved in terms of response time and becomes very fast. On the other hand, the proposed algorithm is developed upon other known algorithms and enhanced in order to identify the occurrence of PSCs and to find the GMPP. The measured points during identification and searching process are reduced which increases the power efficiency of the PV system. The time required for the algorithm to catch the GMPP is minimized by 25% compared with other works. To examine the performance of the system a hard scenario, that contains several uniform and partial shading conditions, is used. The simulation is implemented in Matlab/Simulink. The obtained results show clearly the advantage of the proposed technique over others.

KEYWORDS: PV system, PID controller, PS conditions, GMPPT, PS detection.

[Received Feb. 14, 2023; Revised Nov. 24, 2023; Accepted Dec 12, 2023]

Print ISSN: 0189-9546 | Online ISSN: 2437-2110

I. INTRODUCTION

PV generators are non-linear electric sources. The output power they can deliver, depends on the intersection between the I-V characteristic and the load line. As both of them are variables in time, the intersection point rarely matches the maximum power point (MPP) the generator can produce. For this reason, researchers tried and found solutions by inserting static power converters (DC-DC or DC-AC) between PV generators and loads (Pereira, *et al.*, 2021; Abouchabana, *et al.*, 2021; Osmani, *et al.*, 2021; Rajasekaran, *et al.*, 2020; Morales, *et al.*, 2021) Power converters are controlled by algorithms in order to extract continuously the available MPP (Babes, *et al.*, 2022; Muhammad, *et al.*, 2021; Ameer, *et al.*, 2017).

The efficiency of PV systems depends on many factors such as PV-cells types, converter topologies and MPPT techniques (Hwang, *et al.*, 2021; Ali, *et al.*, 2021; Wang, *et al.* 2021). In recent years, much research has been conducted to improve the PV system's efficiency by proposing new intelligent algorithms that can find and track the MPP under unshaded PV generators (Villegas, *et al.*, 2021; Hossam, *et al.*, 2021; Sarvi, *et al.*, 2021; Jately, *et al.*, 2021; Dadkhah, *et al.*, 2021; Mittal, *et al.*, 2021; Cheng, *et al.*, 2021). When PV generators are partially shaded, P-V characteristic changes significantly its form leading to the appearance of many local maxima. Their greatest value is known as the Global Maximum Power Point (GMPP) (Fares, *et al.*, 2021). In this situation, and depending on the number of

local maxima, only few techniques can find and track the GMPP.

To judge the performance of GMPPT techniques, many criteria are to be considered, such as rapidity, accuracy, stability during the tracking process, partial shading detection, simplicity and cost of implementation (Boukenoui, *et al.*, 2016; Soon, *et al.*, 2015; Kermadi, *et al.*, 2020; Boztepe, *et al.*, 2014).

1) Partial Shading detection

When partial shading happens to PV panels, GMPPT algorithms start a scanning process to find the GMPP. In the majority of algorithms, checking continuously the occurrence of PS is based on the output power change ΔP . Whenever ΔP exceeds a predetermined threshold, the algorithm considers that PS has occurred, and starts a scan of the P-V curve. The strategy of identifying the GMPP differs from one algorithm to another. The time spent for this operation may be short or long. Therefore, triggering an unnecessary scan will lead to power loss and thus affect the algorithm efficiency. This problem may take place when a PV generator is suddenly subjected to a large uniform change in irradiance which make ΔP exceeds the threshold (Kermadi, *et al.*, 2020; Kumar, *et al.*, 2017; Patel, *et al.*, 2008).

2) Rapidity and Accuracy

Both rapidity and accuracy can be adjusted by the MPPT algorithm or/and the regulator used in case of indirect control. Generally, when rapidity is increased, accuracy decreases and

*Corresponding author: b.hadjaissa@lagh-univ.dz

vice versa. This is the case in conventional MPPT algorithms like P&O, Incremental Conductance and others. For large duty-cycle steps, the system responds quickly, but when it reaches the MPP, it oscillates with the same step value resulting in considerable power losses. For small steps, the system takes relatively a long time to get to the MPP, but when it reaches the target, it oscillates with that step resulting in less power loss.

To overcome this problem, other modified algorithms like modified P&O, FL-based algorithm..., have used adaptive step. When the target is far away, the step is large, and when it is close to the target, the step becomes small. Such techniques may miss the GMPP under partial shading conditions (Ahmed, *et al.*, 2021; Belhachat, *et al.*, 2017; Bi, *et al.*, 2020).

When the MPPT algorithm controls directly the power converter in the system, it outputs the duty-cycle. The update of the output duty-cycle must respect the system response time. In PV systems, the response time is dependent on the power converter components (L and C). This means that whatever the algorithm, fast or slow in terms of step size, it is always limited by the system response time.

In case of indirect control, or closed loop control, the MPPT algorithm outputs a reference voltage that will be used as an input for a PID controller (Khaled, *et al.*, 2020). Choosing the voltage as a control variable comes from the fact the MPP voltage is slightly affected by fast irradiance changes. The system response time adjusted and fixed by the user through the PID parameters. This method allows us to speed up significantly the MPP tracking process (Khaled, *et al.*, 2020).

Several research papers carried out to improve the tracking of the GMPP for partially shaded PV generators, however, there is still some issues that can be enhanced in order to make GMPP methods more accurate robust and faster. In this scope, this paper proposes a fast indirect GMPPT method for PV systems under uniform and partial shading conditions.

II. PV SYSTEM CONCEPT

A. System Description

The system used to test the performance of the proposed technique is presented in figure 1. The PV generator is composed of three series-connected panels with two by-pass diodes each. The DC-load is expected to operate at a voltage higher than that of the GMPP, hence the use of a Boost converter.

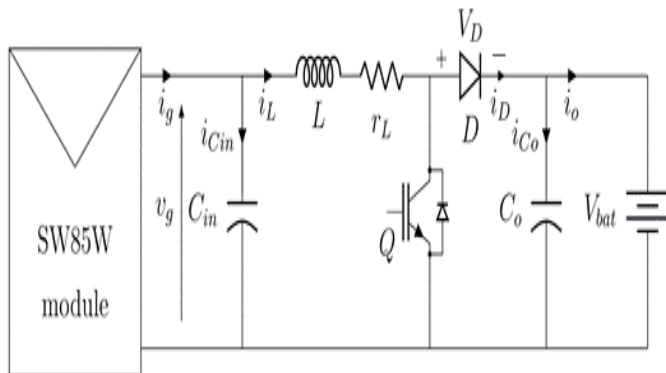


Figure 1: The studied PV system

B. MPPT Indirect Implementation

To implement a MPPT technique, two methods are used: Direct method without voltage regulation loop and indirect method with voltage regulation loop. In the latter, the system charges a controller to calculate the duty cycle as in figure 2.

In the other one, the MPPT algorithm calculates directly the duty cycle without passing by a controller as illustrated in figure 3. The main difference between the two implementations resides in the system response time that will be used to determine at which frequency, f_{mppt} , the MPPT algorithm updates its output. As mentioned in the introduction, in this study we are interested in using PID controller.

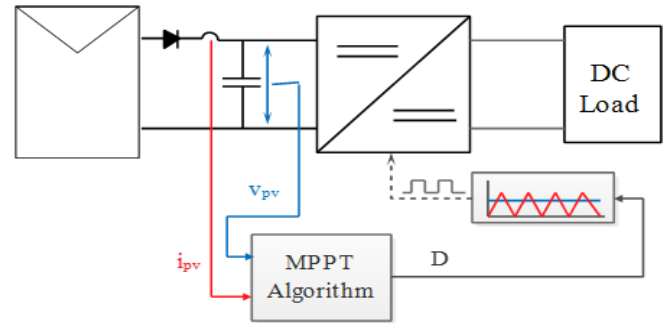


Figure 2: MPPT without voltage closed-loop regulation

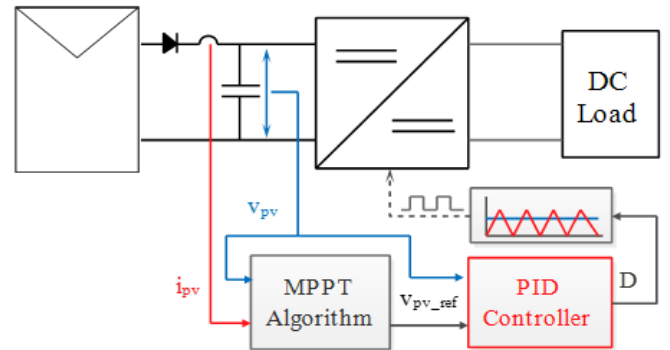


Figure 3: MPPT with voltage closed-loop regulation

C. PV System Modeling

To control a system with classic PID controller, a model is required based on the five-parameter model with one diode, the PV generator is characterized by a non-linear equation. As the system is expected to operate at the vicinity of the MPP point, the PV generator is linearized around that point. The Linear equivalent circuit is illustrated in figure 4. The linearization process is presented in detail in (Khaled, *et al.*, 2020).

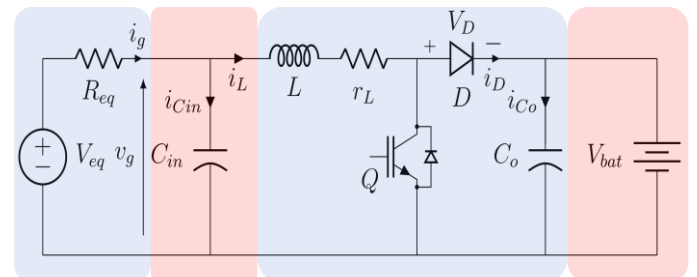


Figure 4: Equivalent circuit of the PV system

1) ON/OFF state model

Over one switching cycle, the system equations can be derived from the on/off-states of the switch Q:

System dynamics when switch Q is in on-state:

$$L \frac{di_L}{dt} = v_g - r_L i_L \quad (1)$$

$$C_{in} \frac{dv_g}{dt} = i_g - i_L = \frac{V_{eq} - v_g}{R_{eq}} - i_L \quad (2)$$

System dynamics when switch Q is in off-state:

$$L \frac{di_L}{dt} = v_g - r_L i_L - (V_d + V_{bat}) \quad (3)$$

$$C_{in} \frac{dv_g}{dt} = i_g - i_L = \frac{V_{eq} - v_g}{R_{eq}} - i_L \quad (4)$$

2) Averaged model

Averaging over one switching cycle, the system equations can be written as follows:

$$L \frac{di_L}{dt} = v_g - r_L i_L - (V_d + V_{bat}) d' \quad (5)$$

$$C_{in} \frac{dv_g}{dt} = \frac{V_{eq} - v_g}{R_{eq}} - i_L \quad (6)$$

Where $d' = (1-d)$ is the control variable.

3) Small signal model

The small signal model is given in the state space form as shown in Eqn. (7):

$$\frac{d}{dt} \begin{bmatrix} \tilde{i}_L \\ \tilde{v}_g \end{bmatrix} = \begin{bmatrix} -\frac{r_L}{L} & \frac{1}{L} \\ -\frac{1}{C_{in}} & \frac{1}{R_{pv} C_{in}} \end{bmatrix} \begin{bmatrix} \tilde{i}_L \\ \tilde{v}_g \end{bmatrix} + \begin{bmatrix} -\frac{V_d + V_{bat}}{L} \\ 0 \end{bmatrix} \tilde{d}' \quad (7)$$

$$\tilde{y} = \begin{bmatrix} 0 & 1 \end{bmatrix} \begin{bmatrix} \tilde{i}_L \\ \tilde{v}_g \end{bmatrix} \quad (8)$$

Applying the Laplace transformation, the small-signal transfer function that relates the small-signal voltage \tilde{v}_g and the control variable \tilde{d}' is given as in (9).

$$G_{vd}(s) = \frac{\tilde{v}_g}{\tilde{d}'} = \frac{K_{vd}}{s^2 \xi_{vd} \omega_{vd} \omega_{vd}^2} \quad (9)$$

Where:

$$K_{vd} = \frac{(V_d + V_{bat})}{C_{in}} \quad (10)$$

$$\xi_{vd} = \frac{r_L R_{pv} C_{in} - L}{2L R_{pv} C_{in} \omega_{vd}} \quad (11)$$

$$\omega_{vd} = \sqrt{\frac{R_{pv} r_L}{R_{pv} C_{in}}} \quad (12)$$

The settling time of the PV system can be obtained using Eqn. (13). When MPPT algorithm is used directly to compute the duty cycle, the minimum time must be waited to see the response of P_{pv} to a change of d , is determined by $T_{st,op}$.

$$T_{st,op} = \frac{\ln(0.02\sqrt{1-\xi_{vd}})}{\xi_{vd} \omega_{vd}} \quad (13)$$

III. PID DESIGN

Figure 5 illustrates the voltage regulation loop of the PV system.

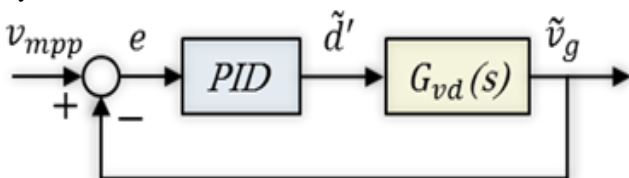


Figure 5: PV system closed loop structure

The closed loop transfer function $T_0(s)$ is given by Eqn. (14), where $G_{vd}(s)$ represents the nominal plant model, $C(s)$ stands for the controller transfer function, $v_{mpp}(s)$ is the control reference, $\tilde{d}'(s)$ symbolizes the control signal, and $\tilde{v}_g(s)$ is the plant output or the control variable (Khaled, *et al.*, 2018).

$$T_0(s) = \frac{\tilde{v}_g(s)}{v_{mpp}(s)} = \frac{C(s)G_{vd}(s)}{1+C(s)G_{vd}(s)} \quad (14)$$

To simplify the design of the controller, a transfer function in terms of the variable $Q(s)$ is introduced as in Eqn. (15). Its closed-loop model representation is illustrated in Figure 6. This simplification permits the transfer function of the closed-loop system to be remodeled as in Eqn. (16).

$$\tilde{d}'(s) = Q(s)v_{mpp}(s) \quad (15)$$

$$T_0(s) = \frac{\tilde{v}_g(s)}{v_{mpp}(s)} = Q(s)G_{vd}(s) \quad (16)$$

The transforming function between $Q(s)$ and $C(s)$ is obtained as in Eqn. (17):

$$C(s) = \frac{Q(s)}{1-Q(s)G_{vd}(s)} \quad (17)$$

For a stable model, it has been confirmed that stability of $Q(s)$ is sufficient to ensure internal stability of the closed loop system (Ameur, *et al.*, 2017).

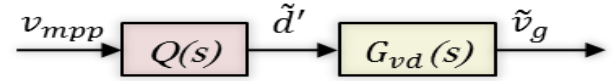


Figure 6: Illustration of Q-parameterization

A. Desired Performance in closed loop

The desired closed-loop transfer function $F_Q(s)$ should be specified from both the damping ratio, which has a relation with the percentage of the overshoot, and the undamped natural frequency, which has relation with the response speed, as in Eqn. (18).

To improve the system performance, the closed-loop parameters are chosen as $\xi_{cl} = 0.7$, $\omega_{cl} = 4.\omega_{vd}$.

$$F_Q(s) = \frac{1}{\frac{1}{\omega_{cl}^2} s^2 + \frac{2\xi_{cl}}{\omega_{cl}} s + 1} = \frac{1}{\alpha_2 s^2 + \alpha_1 s + 1} \quad (18)$$

The settling time can be calculated using the Eqn. (19):

$$T_{st,cl} = \frac{\ln(0.02\sqrt{1-\xi_{cl}})}{\xi_{cl} \omega_{cl}} \quad (19)$$

Then, $Q(s)$ and $C(s)$ are given by Eqns. (20) and (21) respectively.

$$Q(s) = F_Q(s)G_{vd}^{-1}(s) = \frac{s^2 + 2\xi_{vd}\omega_{vd}s + \omega_{vd}}{K_{vd}(\alpha_2 s^2 + \alpha_1 s + 1)} \quad (20)$$

$$C(s) = \frac{Q(s)}{1-F_Q(s)} = \frac{s^2 + 2\xi_{vd}\omega_{vd}s + \omega_{vd}}{K_{vd}s(\alpha_2 s^2 + \alpha_1 s)} \quad (21)$$

The transfer function of the controller can also be expressed in a parallel form as in Eqn.(22)

$$C(s) = K_p + \frac{K_i}{s} + \frac{K_d s}{\tau_d s + 1} \quad (22)$$

Where:

$$\tau_d = \frac{\alpha_2}{\alpha_1}, K_p = \frac{2\xi_{vd}\omega_{vd}\alpha_1 - \alpha_2\omega_{vd}}{K_{vd}\alpha_1^2}, K_i = \frac{\omega_{vd}^2}{K_{vd}\alpha_1} \text{ and}$$

$$K_d = \frac{\alpha_1^2 - 2\xi_{vd}\omega_{vd}\alpha_1\alpha_2 + \alpha_2^2\omega_{vd}^2}{K_{vd}\alpha_1^3} \text{ respectively.}$$

B. Partial Shading Detection Scheme

In this work we have adopted the PS detection scheme presented in (Jubair, *et al.*, 2017; Jubair, *et al.*, 2018). In this scheme, the detection is based on two Eqns. 23 and 24.

$$G_1 = \frac{I_{0.8V_{oc}}}{I_{sc_{STC}}} \cdot G_{STC} \quad (23)$$

$$G_2 = \frac{I_{0.8V_{oc_arr}}}{I_{mpp_{STC}}} \cdot G_{STC} \quad (24)$$

Where $I_{0.8V_{oc}}$ represents I_{sc} in the vicinity of $0.8V_{oc}$, and $I_{0.8V_{oc_arr}}$ is the current I_{mpp} near the voltage $0.8V_{oc_arr}$.

As the PV panel used in our system includes two bypass diodes, V_{oc} symbolizes then the open circuit voltage of only a half panel, and V_{oc_arr} stands for the open circuit voltage of the three series-connected panels.

Under uniform irradiance as illustrated in figure 7, G_1 and G_2 have approximately the same values:

$$G_1 = \frac{2.59}{5.2} \cdot 1000 = 500,9 \text{ W/m}^2,$$

$$G_2 = \frac{2.44}{4.86} \cdot 1000 = 502 \text{ W/m}^2,$$

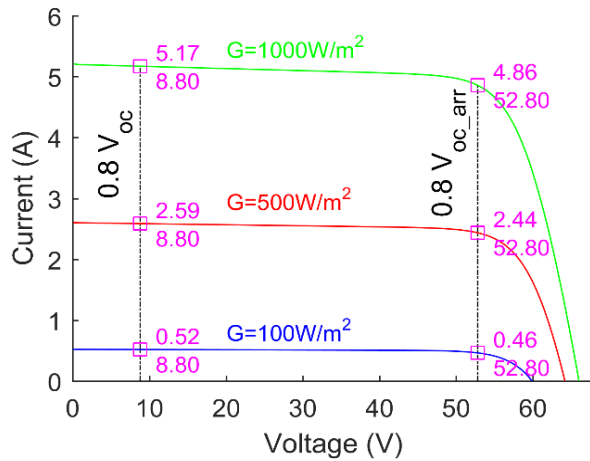


Figure 7: I-V cures under various irradiances for three-series connected panels

The tiny difference between them may differ under different uniform irradiances, but remains below a certain threshold. Figure 8 shows the error $|G_1 - G_2|$ in function of irradiance for the three SW85W PV panels which are used in the studied system.

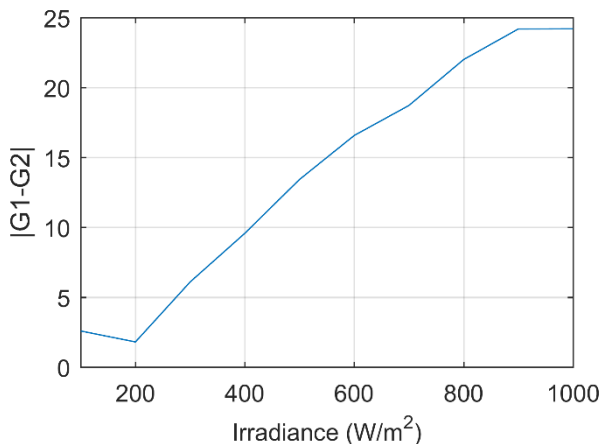


Figure 8: $|G_1 - G_2|$ mismatch vs. irradiance for SW85W PV panel

It can be observed that the error between G_1 and G_2 does not exceed 25 W/m^2 under various uniform irradiances. For this reason, and in order to distinguish between uniform irradiance variation and partial shading occurrence the following equations are used:

$$|G_1 - G_2| < 30 \text{ Means: absence of partial shading} \quad (25)$$

$$|G_1 - G_2| > 30 \text{ Means: occurrence of partial shading} \quad (26)$$

Figure 9 shows different I-V curves under partial shading conditions. Taking as example the red curve, G_1 and G_2 calculation gives:

$$G_1 = \frac{2.96}{5.2} \cdot 1000 = 569,2 \text{ W/m}^2,$$

$$G_2 = \frac{2.03}{4.86} \cdot 1000 = 417.69 \text{ W/m}^2,$$

The absolute difference $|G_1 - G_2| = 151.51 \text{ W/m}^2$, which is much greater than the threshold. In this case, MPPT algorithm identifies easily the partial shading occurrence.

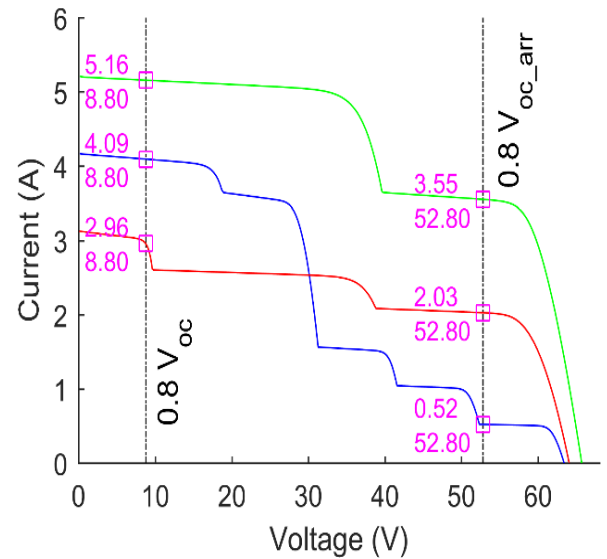


Figure 9: I-V cures under PS for three-series connected panels

C. Updating Open Circuit Voltage V_{oc_arr}

The idea of updating V_{oc_arr} without the need for sensors, which is presented by (Jubair, *et al.*, 2017; Jubair, *et al.*, 2018), brings an important improvement to all Voltage-based MPPT techniques. In addition to the prediction of local maxima bands, it gives continuously the upper limit of the voltage the algorithms must not exceed.

When using meta-heuristic methods to find the GMPP, some information must be provided in order to ensure its convergence, such as the maximum voltage the PV generator can reach. If an algorithm outputs a voltage beyond that maximum, the system will be stuck and try to reach the unreachable voltage. Exploiting the idea of updating V_{oc_arr} without the need for sensors, will help to avoid this situation.

The updating process in (Jubair, *et al.*, 2017; Jubair, *et al.*, 2018) is performed in two steps. In the first step, the authors assumed that the MPP is already tracked under uniform irradiance, and they use a relation between V_{mpp_arr} and V_{oc_arr} in order to find the initial value of V_{oc_arr} , which will be used in the second step. The assumptions they made, make their algorithm

restricted to one initial case, and exclude others. In this work, another idea is proposed to improve the updating process.

In PV systems, where power converters are used to ensure the energy transfer from a PV generator to a load, a capacitor must be connected in parallel with that PV generator. Before the start of the system control, this capacitor is charged by the generator to the open circuit voltage V_{oc_arr} . Its value can be acquired by a simple measurement using a voltage sensor.

Knowing the initial value of V_{oc_arr} help us to avoid the assumption that the MPP is already tracked, which make our algorithm more flexible and includes all possible initial cases. Unlike what is presented in (Jubair, et al., 2017; Jubair, et al., 2018), in this study the updating process is executed as illustrated in figure 10.

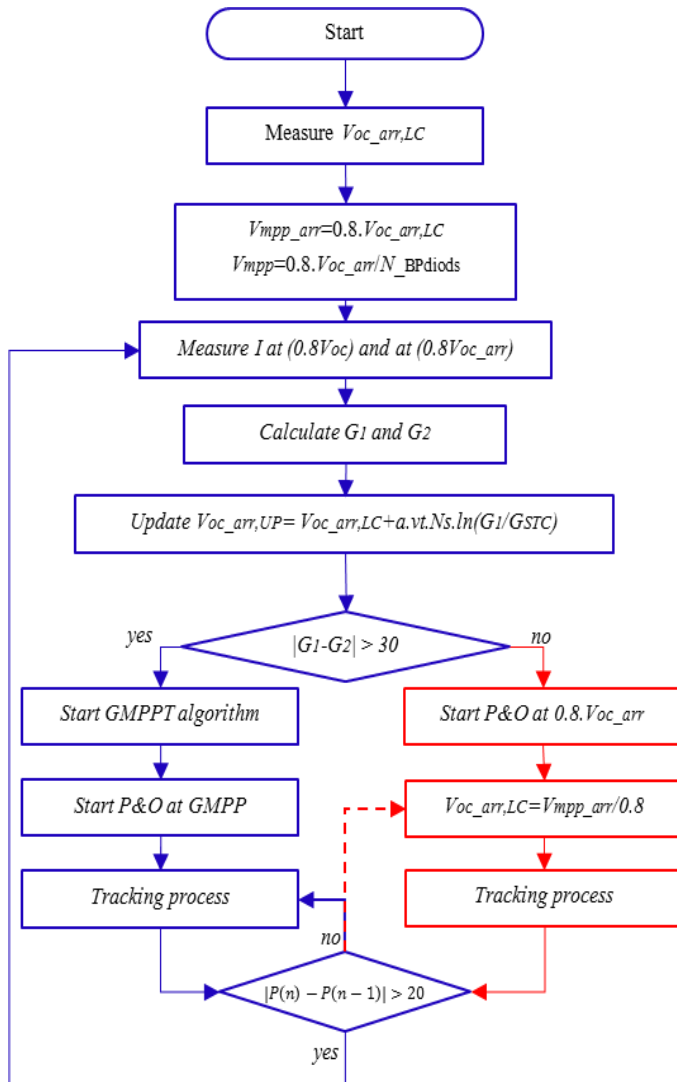


Figure 10: The proposed algorithm

At the beginning, the algorithm measures the open circuit voltage $V_{oc_arr,LC}$. Then, it measures and records the currents $I_{0.8Voc}$ and $I_{0.8Voc_arr}$ in order to calculate G_1 and G_2 . Next, Eqn. (27) is used to update $V_{oc_arr,UD}$. After that, only when the PV generator is under uniform irradiance Eqn. (28) is used:

$$V_{oc_arr,UD} = V_{oc_arr,LC} + a \cdot \left(\frac{ns \cdot k \cdot T}{q} \right) \cdot N_s \cdot \ln \left(\frac{G_1}{G_{STC}} \right) \quad (27)$$

Where $V_{oc_arr,UD}$ is the Updated V_{oc_arr} , a is the diode ideality factor, ns is the number of series-connected cells in one panel, k is the Boltzmann constant, T is the temperature, q is the electron charge, N_s is the number of series-connected panels, and $V_{oc_arr,LC}$ is the Last Calculated value of V_{oc_arr} . At the beginning of the algorithm, $V_{oc_arr,LC}$ is measured across the input capacitor.

$$V_{oc_arr,LC} = \frac{V_{mpp_arr}}{0.8} \quad (28)$$

D. GMPPT algorithm

When a change in power is greater than 10%, the algorithm runs the PS detection routine in which two (02) current values are measured and recorded at $0.8V_{oc_arr}$ and $0.8V_{oc}$ respectively (states 1 and 2 in figure 11).

If PS is not detected, the algorithm goes directly to $0.8V_{oc_arr}$ and runs the P&O algorithm (green arrow in figure 11). In the other case, the algorithm triggers the GMPPT process in which other currents values are to be measured and recorded at voltages multiple of $0.8V_{oc}$ (states 3 to 6 in figure 11), then and after comparison it goes to the voltage at which the power is the greatest and runs the P&O algorithm (blue arrow or red arrow in figure 11).

The GMPPT process does not measure again the current at the checking points; $0.8V_{oc_arr}$ and $0.8V_{oc}$ which make the algorithm faster than that proposed by (Jubair, et al., 2017; Jubair, et al., 2018).

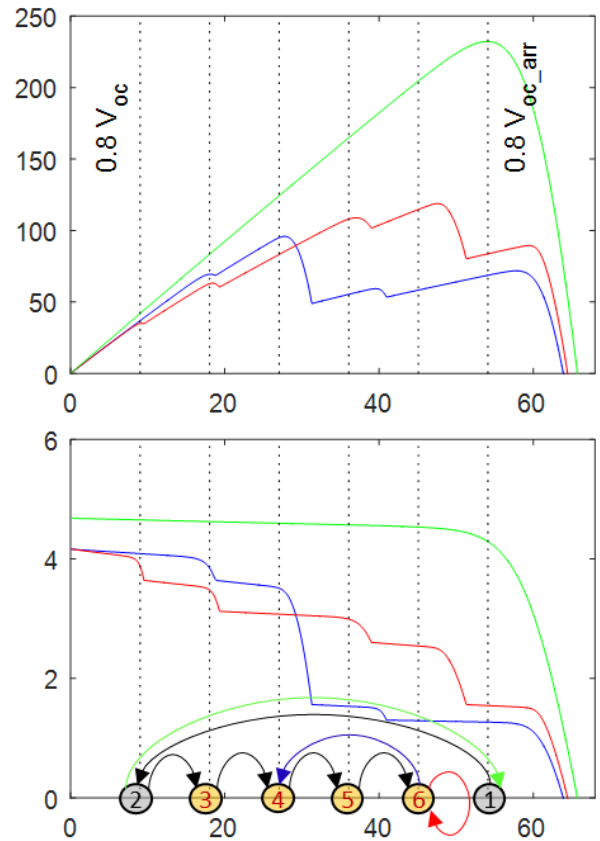


Figure 11: Illustration of the GMPP search process

IV. RESULTS AND DISCUSSION

The PV system used for testing the proposed algorithm is shown in figure 12. It is characterized by: the battery nominal voltage $V_B = 96V$, $f_{SW} = 40$ KHz, $L = 2mH$ with an internal resistance $r_L = 0.15\Omega$, $C_{IN} = 10$ μF and $C_{OUT} = 10$ mF. The PV generator is expected to operate at around $V_{MPP} = 53.7$ V under uniform irradiance. The sample time for the simulation is set as $T_S = 1/40000/100$ (s). The Matlab function block, which contains the GMPPT algorithm, runs every $T_{MPPT} = 1/40000$ (s). To test different algorithms only the Matlab Function block will be changed.

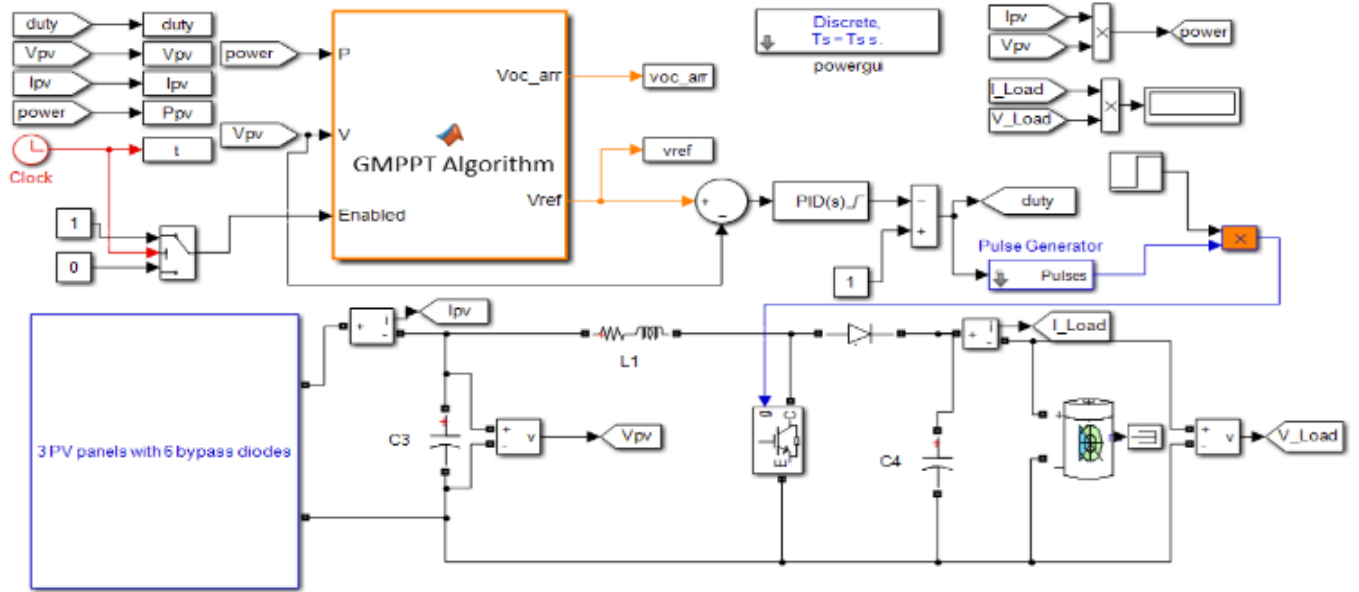


Figure 12: Simulink Model of the studied system

Based on the aforementioned parameters, the settling time of the PV system in open-loop control is given by $T_{(ST_{OP})} = 928.38MS$. With the integration of the PID regulator, the system dynamics is improved and becomes $T_{(ST_{CL})} = 213.17MS$. This means that in order to measure the current at a reference voltage, V_{ref} , the algorithm must wait at least $213.17 \mu s$ to ensure that the PV system has indeed reached V_{ref} , then the algorithm calculates a new reference voltage.

In addition, in the proposed GMPPT algorithm a condition is added, $(V_{ref} - V_m < \epsilon)$, in order to verify each time whether the measured voltage V_m has reached the reference value or not. When the condition $(V_{ref} - V_m < \epsilon)$ is verified, the current is measured and the power is then calculated and the algorithm generates a new reference voltage.

Our proposed algorithm has two advantages;

- 1) Ensuring that the power is calculated at the specified voltage,
- 2) In some cases, the algorithm doesn't need to wait the entire settling time, $T_{st_{cl}}$, (Eqn. 19) in order to measure the current and calculate a new reference voltage. This situation can be noticed in figures 13 to 15. The duration of the reference steps are not equal. Whenever the reference is detected by the algorithm the voltage moves to the new reference, which reduces significantly the duration of the

scanning process and therefore reducing power losses.

The scenario chosen to show the performance of each technique, during 60 ms, is shown in figures 13 to 15. Every 10 ms the PV panels are subjected to different irradiances with sudden change. The P-V curves experienced in each period are drawn in chronological order. The GMPP of each curve is depicted on it as well. It should be noted that both algorithms start working after $1ms$ from the beginning.

Three GMPPT techniques are tested and compared to each other. The first one is based on an adaptive P&O that scans the

integer fraction of $0.8V_{oc_arr}$ and then locate the GMPP as illustrated in figure 13. Whenever the algorithm detects a sudden change in power it triggers the same scan in order to catch the GMPP, except the first one which is executed only at the start-up of the PV system.

Measuring voltage and current is a time-consuming process and making unnecessary measurements leads to more power losses. Looking at the P-V curves in figure 13 (cases 1, 3, 4 and 6), we notice that all PV panels are subjected to uniform irradiance which means that the MPP is located at the vicinity of $0.8V_{oc_arr}$. However, the algorithm triggers a scan of all integer fractions of $0.8V_{oc_arr}$ resulting in excessive power losses.

To overcome this problem, a PS detection scheme is proposed by (Jubair, *et al.*, 2017; Jubair, *et al.*, 2018) and incorporated into the algorithm. Figure 14 shows the results of this technique. When PV panels are exposed to uniform irradiance (cases 1,3,4 and 6) and the algorithm detects a sudden change in power, only two points are measured ($0.8V_{oc}$ and $0.8V_{oc_arr}$) then the algorithm goes back directly to $0.8V_{oc_arr}$ and starts the P&O subroutine.

When partial shading is detected (as in cases 2 and 5) the algorithm, after checking the two points, triggers again a scan of all integer fraction of $0.8V_{oc_arr}$ then it moves to GMPP region and starts the P&O subroutine.

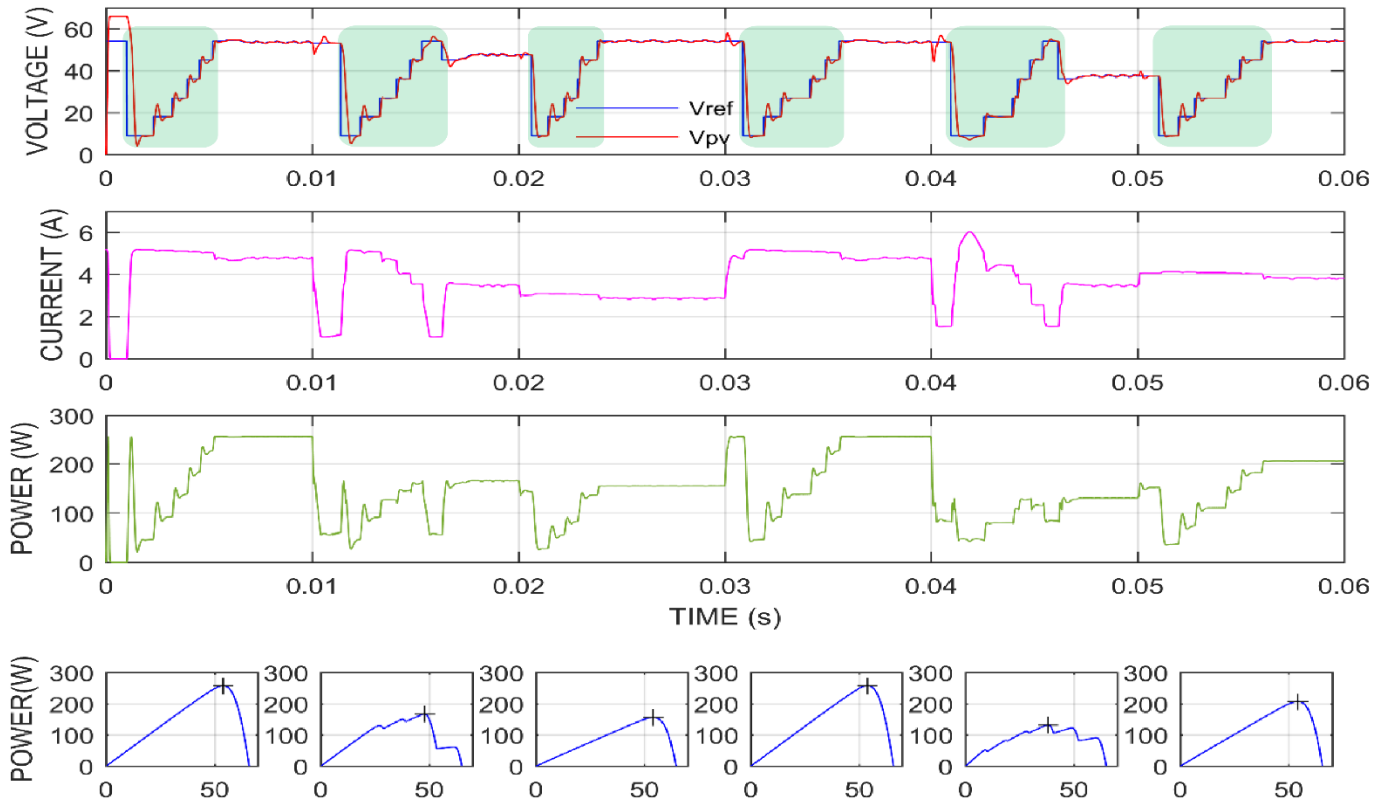


Figure 13: GMPPT algorithm without PS detection scheme

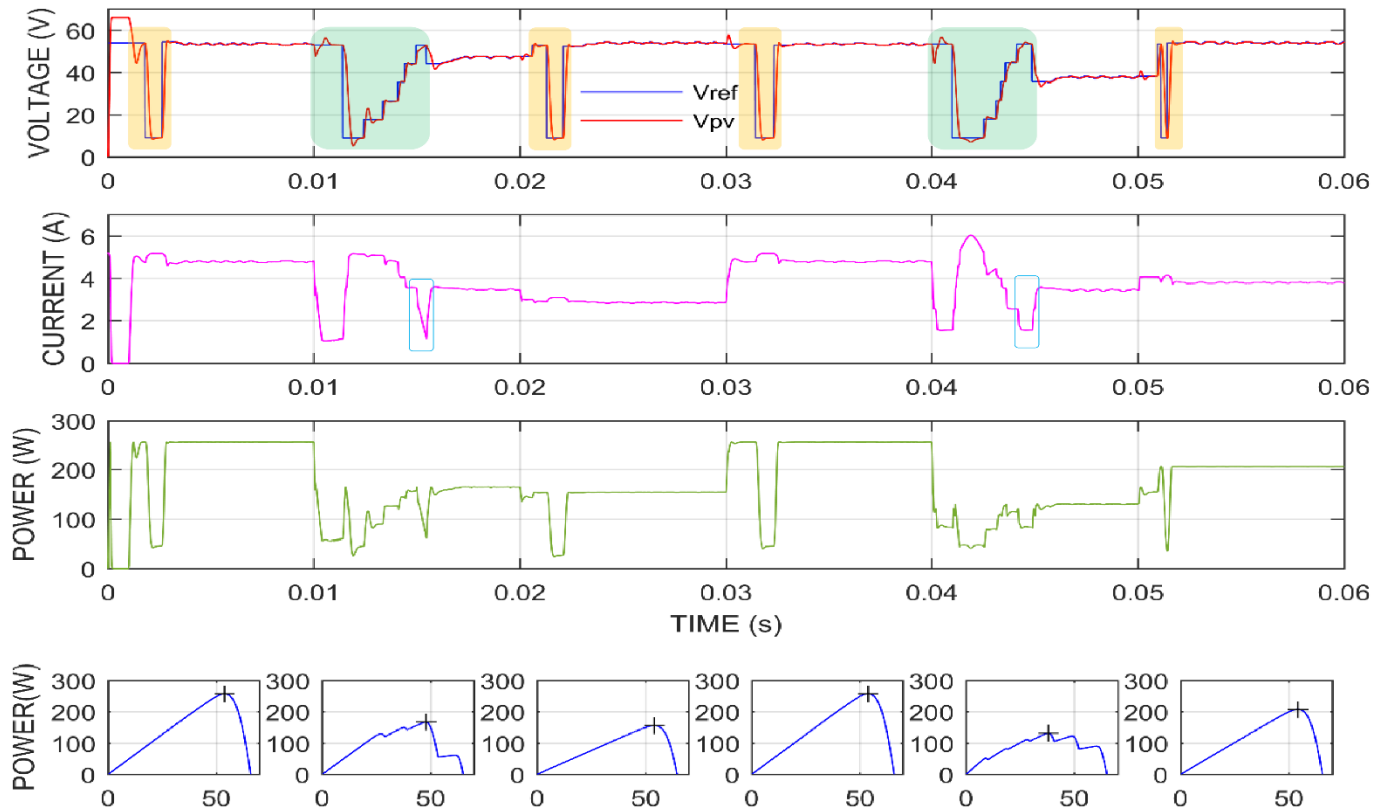


Figure 14: Algorithm of (Jubair, et al., 2017; Jubair, et al., 2018) with PS detection scheme

This algorithm, proposed by (Jubair, *et al.*, 2017; Jubair, *et al.*, 2018), brought a significant improvements to the PV system in terms of power yield compared with the adaptive P&O algorithm. When the algorithm detects a sudden change in power and no Partial Shading (PS) is detected, only two measures are undertaken which saves about 40% of the energy yield that might be lost if algorithm triggers a scan of all integer fractions of $0.8V_{oc_arr}$.

Figure 15 shows the results of the proposed algorithm which incorporated the PS detection scheme as in (Jubair, *et al.*, 2017; Jubair, *et al.*, 2018) but its performance is better than that of (Jubair, *et al.*, 2017; Jubair, *et al.*, 2018) due to the reduced number of measured points during the search of the GMPP.

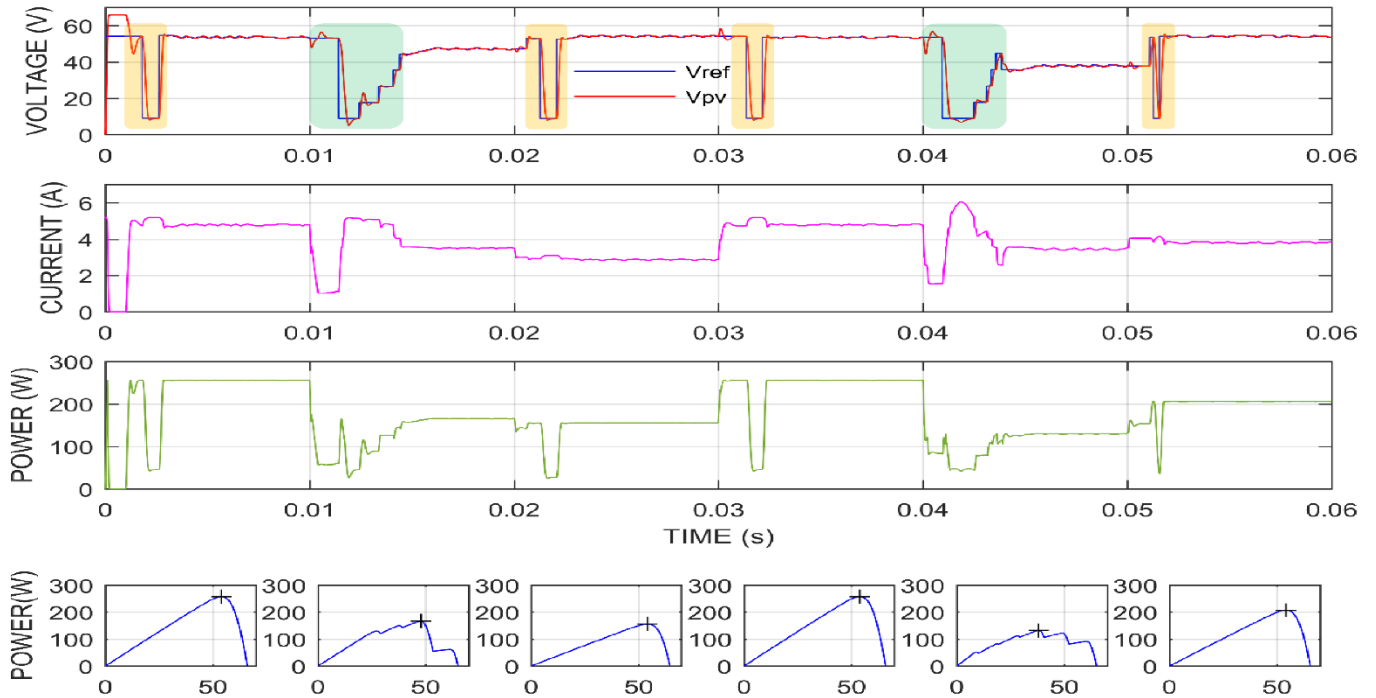


Figure 15: Proposed algorithm with PS detection scheme

Figure 16 shows the main difference between the two algorithms. Under partial shading conditions, both algorithms start measuring the two checking points. When partial shading is detected, the proposed algorithm then measures only the remaining points among those integer fractions of $0.8V_{oc_arr}$, whereas in case of (Jubair, *et al.*, 2017; Jubair, *et al.*, 2018) the checking points are measured again with the other points. We notice in figure 16 that the second checking point ($0.8V_{oc}$) in (Jubair, *et al.*, 2017; Jubair, *et al.*, 2018) algorithm is measured twice but the time needed for that is nearly the same as ours. This happens due to the addition of verification routine ($V_{ref} - V_m < \epsilon$) which allows the algorithm to move to the next point without the need to wait T_{stcl} .

This enhancement brought by the proposed algorithm has reduced the time needed for catching the GMPP from 4, 8 ms to 3, 6 ms, which represent 25% of the GMPPT tracking process.

V. CONCLUSION

In conclusion, this paper has introduced a novel and efficient technique for enhancing the performance of photovoltaic (PV) systems under both uniform and partial shading conditions. The key innovation lies in the implementation of a fast indirect Global Maximum Power Point Tracking (GMPPT) technique, facilitated by the design and incorporation of a Proportional-Integral-Derivative (PID) controller. The PID controller significantly accelerates the system response, achieving a fourfold improvement in comparison to previous methods.

The proposed algorithm, meticulously detailed in this paper, comprises two integral components.

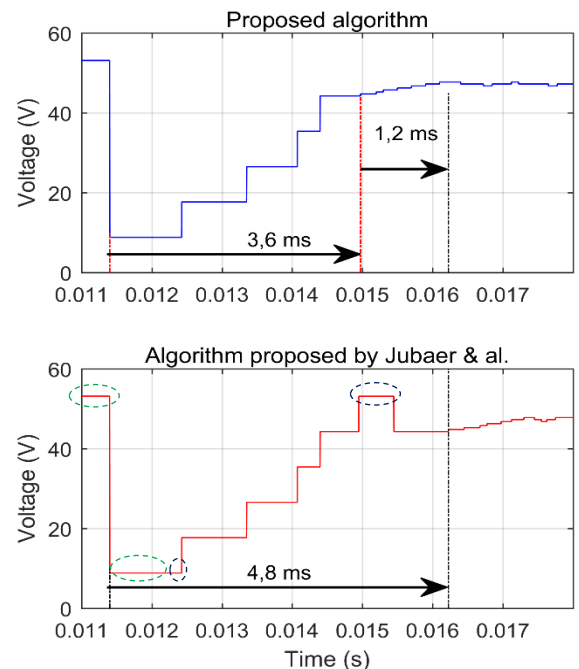


Figure 16: Comparison between the proposed algorithm and the algorithm proposed by Jubair, *et al.*

The first part, inspired by existing literature, focuses on identifying occurrences of partial shading (PS). Subsequently, the second part strategically selects measurement points (voltage and current) based on the outcomes of the first part, ultimately determining the global maximum power point. This two-step approach ensures an optimized and rapid response to varying shading conditions, leading to improved overall system efficiency.

To validate the effectiveness of the proposed technique, comprehensive testing has been conducted under severe scenarios. The simulation results demonstrate the robust capabilities of the algorithm in accurately identifying and tracking the Global Maximum Power Point (GMPP) even in challenging conditions. Furthermore, a comparative analysis with existing works has been performed, highlighting the distinct advantages offered by the presented technique.

In summary, the introduced fast indirect GMPPT technique, coupled with the PID controller, showcases promising advancements in mitigating the impact of shading on PV systems. The demonstrated improvements in speed, accuracy, and adaptability position the proposed method as a noteworthy contribution to the field, providing a valuable tool for enhancing the performance and efficiency of photovoltaic systems in real-world applications.

AUTHOR CONTRIBUTIONS

K. Ameer : Conceptualization, Software, Validation, Writing – original draft. **A. Hadjaissa** : Conceptualization, Methodology, Supervision. **N. Abouchabana and A. Rabhi** : Writing – review & editing.

REFERENCES

- Abouchabana, N.; M. Haddadi; A. Rabhi; A.D. Grasso and G.M. Tina. (2021).** Power Efficiency Improvement of a Boost Converter Using a Coupled Inductor with a Fuzzy Logic Controller: Application of a Photovoltaic System. *Appl.Sci*, 11,980. <https://doi.org/10.3390/app11030980>.
- Ahmed, J; Z. Salam; M. Kermadi; H.N. Afrouzi and R.H. Ashique. (2021).** A skipping adaptive P&O MPPT for fast and efficient tracking under partial shading in PV arrays. *Int Trans Electr Energ Syst*; 31(9):e13017. <https://doi.org/10.1002/2050-7038.13017>.
- Ali, M. N.; K. Mahmoud; M. Lehtonen and M. M. F. Darwish. (2021).** An Efficient Fuzzy-Logic Based Variable-Step Incremental Conductance MPPT Method for Grid-Connected PV Systems," in *IEEE Access*, vol. 9, pp. 26420-26430, doi: 10.1109/ACCESS.2021.3058052.
- Babes, B.; A. Boutaghane and N. Hamouda. (2022).** A novel nature-inspired maximum power point tracking (MPPT) controller based on ACO-ANN algorithm for photovoltaic (PV) system fed arc welding machines. *Neural Comput & Applic* 34, 299–317. <https://doi.org/10.1007/s00521-021-06393-w>
- Bi, Z.; J. Ma; K. Wang; K. L. Man; J. S. Smith and Y. Yue. (2020).** Identification of Partial Shading Conditions for Photovoltaic Strings," in *IEEE Access*, vol. 8, pp. 75491-75502, doi: 10.1109/ACCESS.2020.2988017.
- Boukenoui, R.; H. Salhi; R. Bradai and A. Mellit. (2016).** A new intelligent MPPT method for stand-alone photovoltaic systems operating under fast transient variations of shading patterns, *Solar Energy*, Volume 124, Pages 124-142, ISSN 0038-092X, <https://doi.org/10.1016/j.solener.2015.11.023>.
- Boztepe, M.; F. Guinjoan; G. Velasco-Quesada; S. Silvestre; A Chouder and E. Karatepe. (2014).** Global MPPT Scheme for Photovoltaic String Inverters Based on Restricted Voltage Window Search Algorithm," in *IEEE Transactions on Industrial Electronics*, vol. 61, no. 7, pp. 3302-3312, doi: 10.1109/TIE.2013.2281163.
- Cheng, H.; S. Li; Z. Fan and L. Liu. (2021).** Intelligent MPPT Control Methods for Photovoltaic System: A review," 2021 33rd Chinese Control and Decision Conference (CCDC), pp. 1439-1443, doi: 10.1109/CCDC52312.2021.9602802.
- Dadkhah, J. and Niroomand, M.(2021).** Optimization Methods of MPPT Parameters for PV Systems: Review, Classification, and Comparison," in *Journal of Modern Power Systems and Clean Energy*, vol. 9, no. 2, pp. 225-236, doi: 10.35833/MPCE.2019.000379.
- Dalila. Fares, Mohamed; Fathi, Immad. Shams. and Saad. Mekhilef. (2021).** A novel global MPPT technique based on squirrel search algorithm for PV module under partial shading conditions, *Energy Conversion and Management*, Volume 230, 113773, ISSN 0196-8904, <https://doi.org/10.1016/j.enconman.2020.113773>.
- Faiza, B. and Cherif, L.(2017).** Global maximum power point tracking based on ANFIS approach for PV array configurations under partial shading conditions, *Renewable and Sustainable Energy Reviews*, Volume 77, Pages 875-889, ISSN 1364-0321, <https://doi.org/10.1016/j.rser.2017.02.056>.
- Hossam, H.H. M.; E. Abdel-Raheem Youssef and E.M. Mohamed. (2021).** State of the art perturb and observe MPPT algorithms based wind energy conversion systems: A technology review, *International Journal of Electrical Power & Energy Systems*, Volume 126, Part A, 106598, ISSN 0142-0615, <https://doi.org/10.1016/j.ijepes.2020.106598>.
- Hwang, M.-H.; Kim, Y.-G.; Lee, H.-S.; Kim, Y.-D. and Cha, H.-R.(2021).** A Study on the Improvement of Efficiency by Detection Solar Module Faults in Deteriorated Photovoltaic Power Plants. *Appl. Sc*, 11, 727. <https://doi.org/10.3390/app11020727>
- Jubair, A. and Salam, Z. (2017).** An Accurate Method for MPPT to Detect the Partial Shading Occurrence in a PV System," in *IEEE Transactions on Industrial Informatics*, vol. 13, no. 5, pp. 2151-2161, doi: 10.1109/TII.2017.2703079.
- Jubair, A. and Salam, Z. (2018).** An Enhanced Adaptive P&O MPPT for Fast and Efficient Tracking Under Varying Environmental Conditions," in *IEEE Transactions on Sustainable Energy*, vol. 9, no. 3, pp. 1487-1496, doi: 10.1109/TSTE.2018.2791968.
- Kermadi, M.; Mekhilef, S.; Salam, Z.; Ahmed, J. and Berkouk, E.M.(2020).** Assessment of maximum power point trackers performance using direct and indirect control methods. *Int Trans Electr Energ Syst*; 30:e12565. <https://doi.org/10.1002/2050-7038.12565>
- Kermadi, M.; Salam, Z.; Eltamaly, A.M.; Ahmed, J., Mekhilef, S., Larbes, C. and Berkouk, E.M. (2020).** Recent

developments of MPPT techniques for PV systems under partial shading conditions: a critical review and performance evaluation. *IET Renew. Power Gener.*, 14: 3401-3417. <https://doi.org/10.1049/iet-rpg.2020.0454>

Khaled Ameer; Aboubakeur Hadjaissa; Ali Cheknane and Najib Essounbouli .(2017). DC-Bus Voltage Control Based on Power Flow Management Using Direct Sliding Mode Control for Standalone Photovoltaic Systems, *Electric Power Components and Systems*, 45:10, 1106-1117, DOI: 10.1080/15325008.2017.1318976

Khaled Osmani, Ahmad Haddad, Thierry Lemenand, Bruno Castanier and Mohamad Ramadan. (2021). An investigation on maximum power extraction algorithms from PV systems with corresponding DC-DC converters, *Energy*, Volume 224, 120092, ISSN 0360-5442, <https://doi.org/10.1016/j.energy.2021.120092>.

Khaled, A.; Aboubakeur, H.; Mohamed, B. and Nabil, A.(2018). A Fast MPPT Control Technique Using PID Controller in a Photovoltaic System. *International Conference on Applied Smart Systems (ICASS)*, 2018, pp. 1-5, doi: 10.1109/ICASS.2018.8652062.

Khaled, H. Aboubakeur, A. Nabil and R. Abdelhamid.(2020). Design of a robust PID controller used in PV systems. *1st International Conference on Communications, Control Systems and Signal Processing (CCSSP)*, pp. 370-375, doi: 10.1109/CCSSP49278.2020.9151560.

Kumar, N.; Hussain, I.; Singh, B. and Panigrahi, B. K.(2017). Rapid MPPT for Uniformly and Partial Shaded PV System by Using JayaDE Algorithm in Highly Fluctuating Atmospheric Conditions," in *IEEE Transactions on Industrial Informatics*, vol. 13, no. 5, pp. 2406-2416, doi: 10.1109/TII.2017.2700327.

Morales-Aragón, J.I.; Dávila-Sacoto, M.; González, L.G. and Alonso-Gómez, V.; Gallardo-Saavedra, S. and Hernández-Callejo, L.(2021). A Review of I–V Tracers for Photovoltaic Modules: Topologies and Challenges. *Electronics* 2021, 10, 1283. <https://doi.org/10.3390/electronics10111283>

Muhammad, N. A.; Naim bin Tajuddin, M. F.; Boukenoui, R.; Nalini, C.; Azmi, S. A. and Aziz, A. S.(2021). Investigation on Perturbation Step-Size and Frequency of P&O Algorithm for MPPT under Dynamic Weather Conditions. *Fourth International Conference on Electrical, Computer and Communication Technologies (ICECCT)*, pp. 1-8, doi: 10.1109/ICECCT52121.2021.9616921

Patel, H. and Agarwal, V.(2008). Maximum Power Point Tracking Scheme for PV Systems Operating Under Partially Shaded Conditions," *Industrial Electronics, IEEE Transactions on*, vol. 55, pp. 1689-1698.

Pereira, T. A.; Schmitz, L.; Santos, W. M.; Martins, D. C. and Coelho, R. F.(2021). Design of a Portable Photovoltaic I–V Curve Tracer Based on the DC–DC Converter Method. *IEEE Journal of Photovoltaics*, vol. 11, no. 2, pp. 552-560, doi: 10.1109/JPHOTOV.2021.3049903.

Poornima Mittal, Tarush Goel and Pratyush Gupta.(2021). Evolution of MPPT algorithms in solar arrays, *Materials Today: Proceedings*, Volume 37, Part 2, Pages 3154-3158, ISSN 2214-7853, <https://doi.org/10.1016/j.matpr.2020.09.045>.

Rajasekaran, R and Usha Rani, P .(2020). Bidirectional DC-DC converter for microgrid in energy management system, *International Journal of Electronics*, 108:2, 322-343, DOI: 10.1080/00207217.2020.1793418

Sarvi, M. and Azadian, A.(2021). A comprehensive review and classified comparison of MPPT algorithms in PV systems. *Energy Syst.* <https://doi.org/10.1007/s12667-021-00427-x>

Soon, T. K. and Mekhilef, S.(2015). A Fast-Converging MPPT Technique for Photovoltaic System Under Fast-Varying Solar Irradiation and Load Resistance," in *IEEE Transactions on Industrial Informatics*, vol. 11, no. 1, pp. 176-186, doi: 10.1109/TII.2014.2378231.

Vibhu Jately, Brian Azzopardi, Jyoti Joshi, Balaji Venkateswaran V, Abhinav Sharma and Sudha Arora.(2021). Experimental Analysis of hill-climbing MPPT algorithms under low irradiance levels, *Renewable and Sustainable Energy Reviews*, Volume 150, 111467, ISSN 1364-0321, <https://doi.org/10.1016/j.rser.2021.111467>.

Villegas-Mier, C.G.; Rodriguez-Resendiz, J.; Álvarez-Alvarado, J.M.; Rodriguez-Resendiz, H.; Herrera-Navarro, A.M. and Rodríguez-Abreo, O.(2021). Artificial Neural Networks in MPPT Algorithms for Optimization of Photovoltaic Power Systems: A Review. *Micromachines*, 12, 1260. <https://doi.org/10.3390/mi12101260>.

Wang, Jingwen; Yao, Huifeng; Xu, Ye; Ma, Lijiao and Hou, Jianhui .(2021). Recent progress in reducing voltage loss in organic photovoltaic cells, *Materials Chemistry Frontiers*, vol 5, 2/709-722, <https://doi.org/10.1039/DOQM00581A>.